ARTICLE

Cavity Ring-Down Spectroscopy Measurements of Ambient NO_3 and N_2O_5[†]

Hao Wu[a], Jian Chen[b], An-wen Liu[b], Shui-ming Hu[a,b*], Jing-song Zhang[c]

a. Hefei National Laboratory for Physical Sciences at the Microscale, University of Science and Technology of China, Hefei 230026, China
b. Department of Chemical Physics, School of Chemistry and Materials Science, University of Science and Technology of China, Hefei 230026, China
c. Department of Chemistry and Air Pollution Research Center, University of California, Riverside California 92521, USA

(Dated: Received on October 6, 2019; Accepted on December 2, 2019)

NO_3 and N_2O_5 are important participants in nocturnal atmospheric chemical processes, and their concentrations are of great significance in the study of the mechanism of nocturnal atmospheric chemical reactions. A two-channel diode laser based cavity ring-down spectroscopy (CRDS) instrument was developed to monitor the concentrations of NO_3 and N_2O_5 in the atmosphere. The effective absorption length ratio and the total loss coefficient of the instrument were calibrated using laboratory standard samples. The effective absorption cross section of NO_3 at 662 nm was derived. A detection sensitivity of 1.1 pptv NO_3 in air was obtained at a time resolution of 1 s. N_2O_5 was converted to NO_3 and detected online in the second CRDS channel. The instrument was used to monitor the concentrations of NO_3 and N_2O_5 in the atmosphere of winter in Hefei in real time. By comparing the concentration changes of pollutants such as nitrogen oxides, ozone, $PM_{2.5}$ in a rapid air cleaning process, the factors affecting the concentrations of NO_3 and N_2O_5 in the atmosphere were discussed.

Key words: Cavity ring-down spectroscopy, Nitrate radical, Dinitrogen pentoxide, Field measurement

I. INTRODUCTION

Nitrate radicals (NO_3) and dinitrogen pentoxide (N_2O_5) are important components of atmospheric nitrogen oxides. They are produced by oxidation of low valence state nitrogen oxides in the atmosphere (Eq.(1)) and they are important participants in the atmospheric chemical reactions.

$$\begin{aligned} &NO + O_3 \rightarrow NO_2 + O_2 \\ &NO_2 + O_3 \rightarrow NO_3 + O_2 \\ &NO_2 + NO_3 \leftrightarrow N_2O_5 + O_2 \end{aligned} \quad (1)$$

The nitrate radical has a high reactivity, and furthermore it can be readily photolyzed under solar radiation, leading to a short life time [1]. As a result, the concentration of NO_3 during the daytime is very low, and it only exists at night [2]. As one of the important oxidants in the atmospheric oxidation reactions at night, NO_3 is involved in the oxidative degradation of various atmospheric pollutants (such as VOCs [3], sulfide [4], *etc.*).

In the atmosphere, dinitrogen pentoxide (N_2O_5) is mainly produced by the reaction between the nitrate radical and nitrogen dioxide in a chemical equilibrium among them (Eq.(1)), which makes N_2O_5 as a reservoir of the NO_3 radical in the atmosphere. Besides the transformation to the nitrate radical, hydrolysis reaction of N_2O_5 involving aerosol particles, clouds and fog is another significant loss pathway [5–7]. Nitric acid and nitrate produced by this reaction are one of the main sources of nitrate in the atmosphere [2, 8, 9].

The concentrations of the nitrate radical and dinitrogen pentoxide in the atmosphere are both at the level of parts-per-trillion by volume (pptv) [5, 10]. Therefore, the measurement technique should have a high sensitivity and selectivity. N_2O_5 can be detected indirectly through the detection of NO_3 following the thermal decomposition of N_2O_5. After Noxon *et al.* [11] first detected NO_3 in the tropospheric atmosphere by differential optical absorption spectroscopy (DOAS) in 1978, a variety of techniques have been developed to detect NO_3 in the subsequent 40 years, among which spectroscopy and mass spectrometry methods were frequently applied. The most commonly used mass spectrometry method is chemical ionization mass spectrometry, and its detection limit can reach 11 pptv [12]. Matrix-isolation electron spin resonance spectroscopy (MI-ESR) has very high selectivity in detecting NO_3, which can be used for highly sensitive off-line measure-

[†]Part of The special topic on "The 3rd Asian Workshop on Molecular Spectroscopy".
*Author to whom correspondence should be addressed. E-mail: smhu@ustc.edu.cn

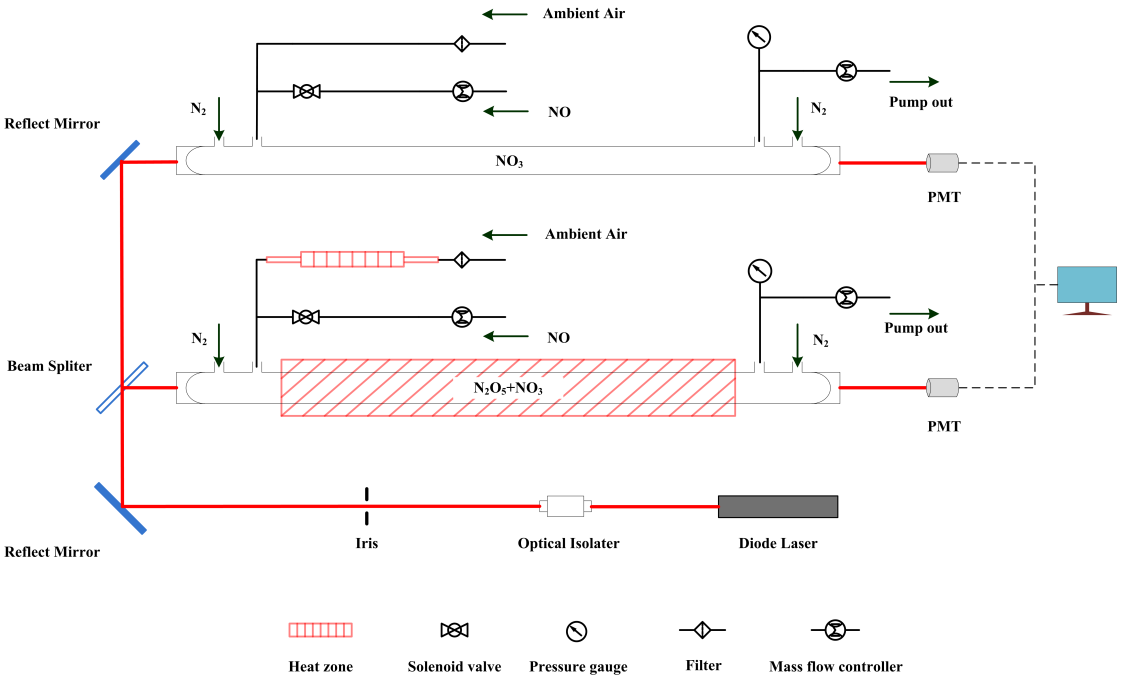

FIG. 1 Experimental setup.

ment of the NO_3 radical [13, 14]. However, MI-ESR needs a complicated and time-consuming sample collection and detection procedure, which limits its wide application.

NO_3 can be detected through its strong absorption around 623 nm and 662 nm. The laser induced fluorescence (LIF) technique was applied for a quantitative measurement of NO_3 by measuring the fluorescence in the 700−750 nm region emitted by NO_3 after absorption of the 662 nm photon, and the reported detection limit reached 6 pptv (1σ, 10 min) [15]. The DOAS technique uses sunlight and moonlight for passive measurement, enabling a global measurement [16] and a determination of NO_3 concentration in the stratospheric atmosphere [17]. Alternatively, high sensitivity can be achieved through active measurement by using laboratory light source, which resulted in a detection limit of 2 pptv [18]. Using laser light travelling back and forth multiple times inside an optical resonator composed of two highly reflective mirrors, cavity enhanced absorption spectroscopy (CEAS) and cavity ring-down spectroscopy (CRDS) techniques obtain a very long effective absorption path length and enhance the detection sensitivity. The detection limit of CEAS can reach 2 pptv [19], and the sensitivity of CRDS can reach 1 pptv [20]. In China, a few groups from Peking University [21], Fudan University [22], Anhui Institute of Optics and Fine Mechanics [23] and Hong Kong Polytechnic University [24] reported the detection of NO_3 and N_2O_5 using different methods such as DOAS, CEAS, and CRDS. In this study, we present a dual-channel CRDS instrument based on diode lasers for the detection of ambient NO_3 and N_2O_5. As a demonstration, the instrument was used to monitor concentrations of the nitrogen oxides during a rapid air cleaning process.

II. EXPERIMENTS

A. Experimental techniques

A two-channel cavity ring-down spectrometer was used for real-time online analysis of the ambient samples. The basic principle is to place the sample gas in an optical resonant cavity consisting of a pair of high-reflection (HR) mirrors. A continuous-wave laser was coupled into the optical cavity and traveled many times inside the cavity until a stable light field was formed. When the incident laser was turned off, the light field in the cavity gradually decreased due to the transmission and loss of the mirrors, as well as the absorption and scattering by the gas sample, which resulted in an exponential decay of the transmitted light intensity. By fitting the decay curve, one can derive the relationship between the absorption coefficient α and the ring-down time τ:

$$\alpha(\nu) = \frac{1}{c\tau(\nu)} - \frac{1}{c\tau_0(\nu)} \tag{2}$$

where c is the speed of light, and $\tau(\nu)$ and $\tau_0(\nu)$ are ring-down times with and without the sample, respectively. The configuration of our experimental setup is shown in FIG. 1.

DOI:10.1063/1674-0068/cjcp1910173

Our optical cavity was constructed with a pair of HR mirrors (R≈99.996%) positioned about 87 cm apart. The sample cell was made by 3/4 inch outer diameter (O.D.) and 5/8 inch inner diameter (I.D.) PFA tube. The inlet and outlet of the gas sample were between the HR mirrors at a distance of 45 cm (see in FIG. 1). A 662 nm diode laser (IQu Series, PTI) with a maximum output power of 120 mW was used as the light source for both optical cavities (with a 50/50 split). Square wave signal generated by a function generator switched the laser at a frequency of 1 kHz. An optical isolator was used to prevent the reflected light from windows and HR mirrors from affecting the laser output. A photomultiplier tube (PMT, H10721-20, Hamamatsu) was used for signal detection. To avoid the influence of stray light, a narrow-band high-efficiency optical band-pass filter was placed in front of the PMT. The signal collected by the PMT was amplified by a signal amplifier and digitized via an analog-digital conversion card (PCI 9820, ADLink) and processed by a personal computer. Ring-down events were recorded and averaged for typically one second to improve the signal-to-noise ratio.

For each CRDS channel, a 5 μm-pore polytetrafluoroethylene membrane (TE 38, Whatman, GE) was used to filter out particles in the air sample. Air sample was pumped into the CRDS cavity by a diaphragm pump through a 1/4 inch O.D. sampling tube (PFA) after the filter. The injection rate was controlled by mass flow controller (MFC). To avoid the loss of the measured object in the MFC and diaphragm pump, both of them were placed at the outlet of the cavity air path, and the flow rate of MFC was controlled at 4.15 slpm (standard liter per minute). At the same time, in order to protect the surface of the high reflection mirror from being contaminated by the atmospheric samples, 75 sccm (standard cubic centimeter per minute) high-purity nitrogen gas was injected at the surface of each HR mirror as the protective gas. As shown in FIG. 1, one of the CRDS channels was used for direct measurement of the atmospheric concentration of the NO_3 radicals, and the second channel was fed with sample gas through a membrane along with the teflon tube heated to 120 °C, which converted the ambient N_2O_5 completely (99.6%) to NO_3 with a ratio of 1:1. In the second channel, the CRDS cavity was kept at temperature of 80 °C and also measured the NO_3 concentration. The N_2O_5 concentration in the air sample was derived from the difference between the NO_3 concentrations measured by the two CRDS channels.

B. Calibration

The high reactivity of the NO_3 radical makes its loss during the sampling and measurement processes inevitable. In order to obtain the concentration of NO_3 in the air sample more accurately, a series of measurements were carried out to calibrate the related coefficients.

First, by comparing the ring-down time τ with the sample and τ_0 without the sample (zero gas), the sample absorption coefficient α was obtained (Eq.(2)). Then the volume concentration of NO_3 was determined according to Eq.(3),

$$\chi = \frac{\alpha(\nu)}{\sigma(\nu)} \times \frac{R_{\mathrm{L}}}{1-\eta} \times \frac{RT}{PN_{\mathrm{A}}} \tag{3}$$

where $\sigma(\nu)$ is the absorption cross section of NO_3, R_{L} is the ratio of the optical cavity length to the absorption path length of the sample, η is total loss coefficient of the NO_3 sample in the apparatus, N_{A} is Avogadro constant, R is the gas constant, T is the sample temperature in K, and P is the gas pressure.

The ratio R_{L} was introduced because the N_2 purge gas was used in the measurement to protect the HR mirrors at both ends of the cavity, so that the sample gas absorption path length was less than the total cavity length between the two HR mirrors. This coefficient was related to the geometry of the cavity and the flow rates of the sample gas and protection N_2 gas. This coefficient was calibrated using a system for the NO_2 detection which had the same configuration as this one. The R_{L} coefficient in the NO_2 system was calibrated by comparing the NO_2 concentration measured by CRDS and that by a commercial NO_x analyzer (42i-TL, Thermo Fisher Scientific), which gave R_{L}=1.54±0.02 [25]. Since the same experimental conditions were applied in the NO_3 measurement, this R_{L} coefficient was used for the NO_3 apparatus.

The loss of NO_3 was mainly due to sampling tubing, cavity wall, and surface of the filter membrane. The porous structure of the membrane not only filtered aerosol, but also led to a loss of NO_3 in the sample gas. It was therefore necessary to measure the loss of NO_3 before its detection by CRDS. A standard NO_3 sample was used to calibrate the loss ratio. By slowly passing the high-purity nitrogen gas through a solid state N_2O_5 sample stored in a dry ice-alcohol mixture bath with a flow rate of 25 sccm, a sample of N_2O_5 with a stable concentration was obtained. After high-temperature pyrolysis (∼120 °C), the N_2O_5 sample was converted to a stable flowing sample of NO_3.

Two gas inlet channels were used to determine the loss ratio due to the membrane filter. These two channels were identical except that the membrane filter was installed in one of them. The sample gas was flown into the CRDS measurement cavity and switched between the two gas inlet channels. The NO_3 concentration detected by CRDS is shown in FIG. 2. Besides a steady drift of the NO_3 concentration due to the change of the source sample, a difference between the two curves measured through these two inlet channels with and without the membrane filter was clearly identified. The difference gave a loss ratio of (13±2)% due to the membrane filter.

The transmission loss was determined by two methods, similar to those by Dube *et al.* [26] and Fuchs *et*

DOI:10.1063/1674-0068/cjcp1910173

al. [27]. The first was to measure the linear loss rate of the NO_3 radical in our sample tube. By pumping the sample into a 40 cm, 1/4 inch teflon tube at different rates, 1.5 slpm, 2.5 slpm, 3.5 slpm and 4.5 slpm, through a sample tubing volume of about 50 mL from the inlet tube to the center of the CRDS sample cell, residence time of the prepared NO_3 sample inside our device was obtained as 2.0 s, 1.2 s, 0.86 s, and 0.67 s respectively. With a linear fitting of the measured concentration of NO_3 to the residence time, the transmission loss rate can be determined as (11±2)%. In our monitoring process, considering the length of the inlet tubing, the transmission loss was determined as (14±2)%.

The second was to measure the loss directly in our device. The prepared NO_3 sample was converted to NO_2 by mixing with the excessive NO gas, and the concentration of the NO_2 product was measured by the CRDS instrument for the NO_2 detection [25], which quantified the concentration of the NO_3 sample. By comparing the NO_3 concentrations measured under the experimental conditions that sample tubing of different lengths were used, the loss ratio of NO_3 during the transportation in sample tubing and the cavity wall was also determined, which was (12±2)%. This process utilized an extra device which could introduce additional uncertainty; as a result, we decided to use the result of the first process for our calibration procedure.

Finally, the total loss ratio of NO_3 was obtained from a combination of the filter loss and transmission loss, and in our experiment apparatus it was determined to be η=(27±3)%.

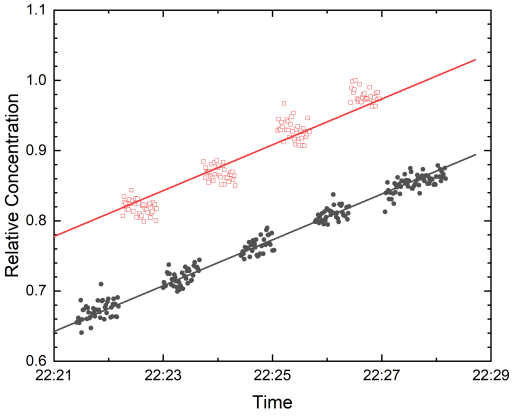

FIG. 2 Loss rate of the NO_3 radical by measuring the relative concentration of the NO_3 standard sample with and without the 5 μm filter in the inlet gas path. Data shown in black and red are measured with and without the filter, respectively.

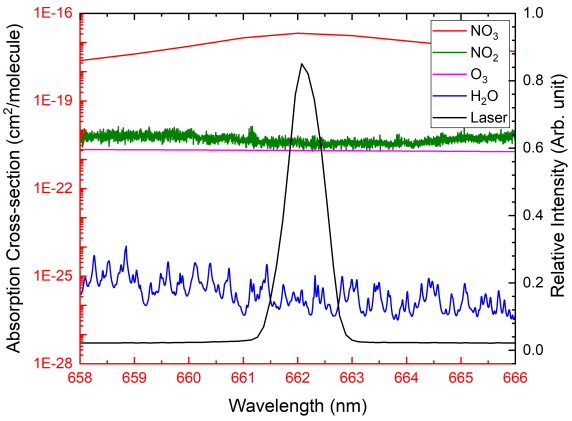

FIG. 3 Absorption cross sections of NO_3, NO_2, O_3, H_2O and emission spectrum of the diode laser.

III. RESULTS AND DISCUSSION

A. Measurement performance

In order to improve the measurement sensitivity and signal-to-noise ratio and avoid the interference due to other molecules in the air sample, the laser center frequency used in the measurement was selected to be near the peak of the absorption of NO_3 at about 662 nm. The black line in FIG. 3 is the emission spectrum curve of the diode laser measured by a grating spectrometer (Shamrock 750) with a resolution of 0.5 nm. The center of the laser emission was determined to be 662.07 nm. By convolving the laser emission spectrum with the NO_3 absorption cross section curve at 298 K (red line in FIG. 3) [28], an effective absorption cross section of NO_3 at 662.07 nm was determined to be 2.04×10^{-17} $cm^2molecule^{-1}$.

Optical extinction due to components other than NO_3 in the atmosphere may affect the measurement: such as Rayleigh scattering of nitrogen and oxygen, Mie scattering of aerosol particles, and absorption of water vapor, ozone and nitrogen dioxide. During the measurement, the mass flow controller ensured that the pressure in the cavity was kept within a range of 1% atm, and therefore the Rayleigh scattering effect can be considered as a constant contribution to the baseline which could be directly removed. The membrane filter placed in the sample inlet channel filtered out most aerosol particles in the sample gas, which reduced the influence of Mie scattering of aerosol particles.

The resonant absorption at 662 nm of some trace gas molecules in the atmosphere could also influence the measurements, especially the water vapor [29], ozone [30] and nitrogen dioxide [31]. FIG. 3 shows the absorption cross sections of the three molecules as well as NO_3 around 662 nm [32]. Note that the absorption cross sections of H_2O, O_3 and NO_2 are three to nine orders of magnitude smaller than that of NO_3. However, since the concentration of NO_3 in the atmosphere is at the pptv level, much lower than those of interfering molecules, it was necessary to consider the influence due to each interfering molecule in the atmosphere. Taking the typical concentrations in the atmosphere such as 30 ppbv for nitrogen dioxide, ozone 30 ppbv, water vapor

DOI:10.1063/1674-0068/cjcp1910173

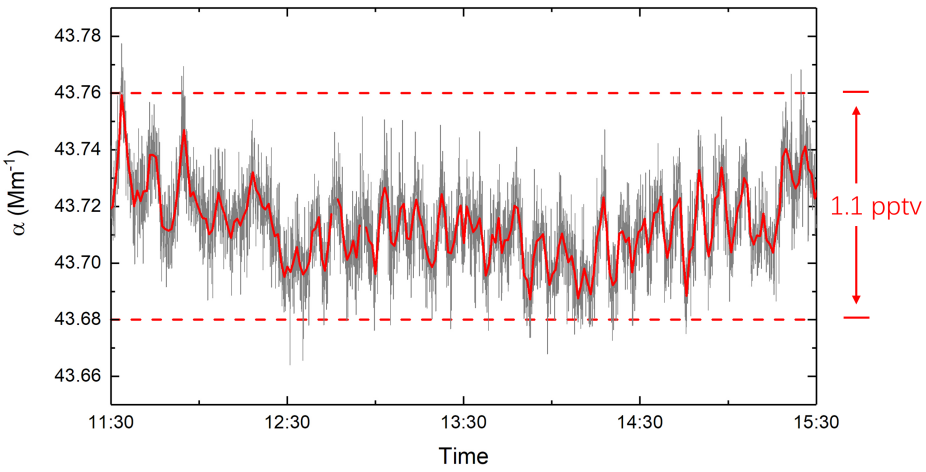

FIG. 4 Absorption coefficient α of zero air measured in a 4-h period.

1%, and combining with the absorption cross sections of these molecules at the wavelength of the laser used in our measurement, the contribution from each molecule can be converted and scaled in terms of the NO_3 concentration. They were NO_2 10.4 pptv, O_3 4.0 pptv, and H_2O 5.1 pptv. Therefore, the interferences of these three molecules were not negligible.

In order to eliminate their interferences, 6 ppmv nitric oxide gas was repeatedly injected into the sample gas at a 100 sccm flow rate, and the difference of CRDS absorption coefficient ($\Delta\alpha$) was measured. Since NO converted NO_3 and O_3 to NO_2, the absorption due to NO_3 decreased 3 orders of magnitude after the NO_3 to NO_2 conversion and that due to O_3 increased 2 times from O_3 to NO_2 conversion, thus the change $\Delta\alpha$ would be predominantly related to the concentrations of NO_3 and O_3 in the sample, eliminating the influence due to NO_2 and water vapor in the sample. The change $\Delta\alpha$ due to the presence of O_3 was relatively small and the influence can be further corrected if the O_3 concentration was known.

In atmospheric monitoring, the measurement results are often influenced by environmental conditions such as temperature and air pressure. In order to examine the sensitivity and stability of the device, a continuous measurement of 4 h using zero air under the same experimental conditions was conducted. The results are shown in FIG. 4, where the gray curve was obtained with a time resolution of 1 s, and the red curve was with a time resolution of 3 min. During the 4-h measurement, the peak-to-peak fluctuation in the absorption coefficient was 8×10^{-10} cm^{-1}, which corresponded to a NO_3 concentration of 1.1 pptv. It could be used as the detection sensitivity (3σ) of NO_3 of this instrument.

B. Field measurement

As a demonstration, the instrument was applied in a continuous measurement of the outdoor air for a week from November 1, 2017 to November 7, 2017. The sampling site of this measurement was selected in the Science and Technology Building of University of Science and Technology of China in Hefei, Anhui Province. The sampling port was about 8 m away from the ground and 1 m away from the wall. It was about 100 m away from the Huangshan road, one of the main thoroughfares in Hefei city. The road had a large traffic flow during morning and evening rush hours, and the air samples taken in this area could be regarded as a typical urban pollution sample in the winter season.

Together with the NO_3 and N_2O_5 measurements, another CRDS instrument operating at 405 nm [25] was also applied to monitor the concentration of NO_2 in the atmospheric sample. The concentrations of $PM_{2.5}$ and O_3, temperature and humidity given from the Hefei city meteorological monitoring station were also recorded, in order to understand the environmental factors related to the concentration changes of NO_3 and N_2O_5 in the atmosphere. The results are shown in FIG. 5. The NO_3 and N_2O_5 data were averaged with a time resolution of 90 s and the NO_2 signal was averaged for 180 s. The $PM_{2.5}$, O_3, temperature and humidity data were only available with a time resolution of 1 h.

It is noted that NO_3 and N_2O_5 were only produced after sunset, and their concentrations during the daytime were below our detection limit, so our measurements of NO_3 and N_2O_5 were carried out only at night. The yellow background in FIG. 5 indicates the daytime period, and the white background is for the night period. It can be seen that during the entire measurement, the N_2O_5 concentration had a few peaks of about 10−20 pptv, while the concentrations of NO_3 stayed lower than 2 pptv. Only around 00:00 on November 5, when N_2O_5 showed a persistent high concentration, the NO_3 concentration had an obvious peak lasting for about 2 h.

In fact, the concentrations of NO_3 and N_2O_5 in the atmosphere were the result of the interaction of vari-

DOI:10.1063/1674-0068/cjcp1910173

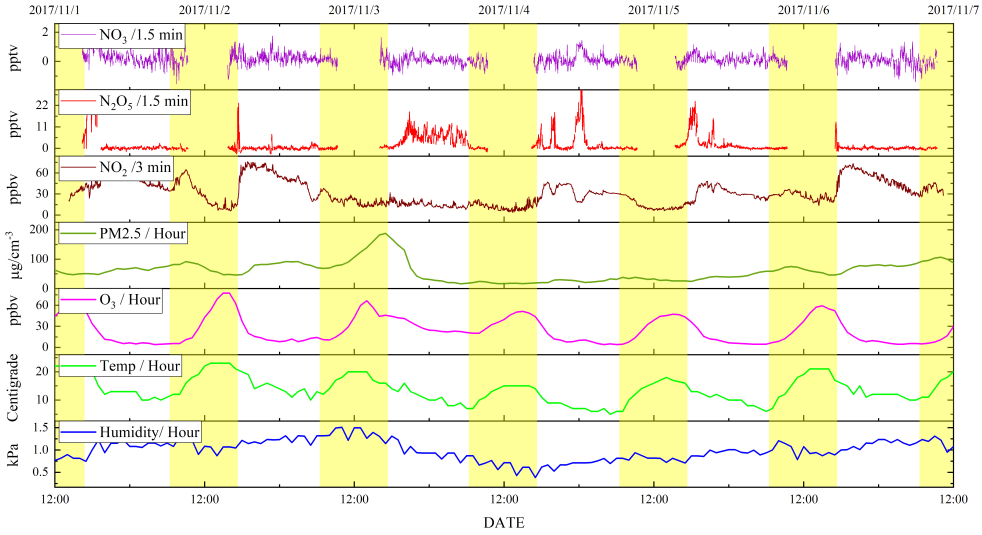

FIG. 5 Ambient measurements of atmospheric pollutants. Yellow areas indicate the day time between sunrise and sunset.

ous atmospheric conditions. As a short-term continuous monitoring, only the relatively obvious and typical events were selected for analysis, giving rise to a preliminary correlation analysis.

As shown in FIG. 5, when N_2O_5 reached a peak concentration, NO_2 concentration always came to a minimum. The correlation was more apparent when the concentration of N_2O_5 peaked during the night from November 4 to November 5 and the night from November 5 to November 6, which was consistent with the reaction mechanism (Eq.(1)). It was also noticed that there was a small O_3 peak during the night of November 4. A possible interpretation is that N_2O_5 produced in the atmosphere at this time was from the production of NO_3 by O_3 oxidation of NO_2 and then formation of N_2O_5 by combining NO_3 and NO_2.

A special atmospheric process observed in this measurement was that after the accumulation of $PM_{2.5}$ during the daytime of November 3, it was quickly cleared in the night of November 3 and kept a low concentration in the following days. By comparing the measurement results of N_2O_5 before and after the sudden drop in the $PM_{2.5}$ concentration, it can be seen that low $PM_{2.5}$ concentration appeared to be a prerequisite for the presence of N_2O_5. When the $PM_{2.5}$ concentration was high, the N_2O_5 concentration was low, which may be due to that the aerosol particles provided more reaction surface for NO_3 and considerably reduced the lifetime of NO_3 in the atmosphere.

It can also be seen from FIG. 5 that the concentration of N_2O_5 after November 3 was higher than that of the previous two days, correlated with a low humidity during the same period. However, since the decrease of $PM_{2.5}$ was also related to the decrease of humidity, it was difficult to determine whether humidity or $PM_{2.5}$ concentration played a key role in the change of the N_2O_5 concentration, which requires further investigation.

IV. CONCLUSION

A dual-channel cavity ring-down instrument based on diode lasers using the 662 nm absorption band of NO_3 was developed for measurements of NO_3 and N_2O_5 in the atmosphere. A NO_3 detection sensitivity of 1.1 pptv (3σ) was demonstrated. The possible interference due to other substances in the atmosphere, such as NO_2, O_3, and water was discussed. After calibration of the instrument with laboratory NO_3 standard sample, the NO_3 and N_2O_5 concentrations in the atmosphere can be simultaneously determined quantitatively at a precision better than 1 pptv. Using this instrument, together with another CRDS instrument for the NO_2 detection, a field measurement lasting for 1 week was carried out by measuring NO_3, N_2O_5 and NO_2. Combining with the meteorological data of ozone, $PM_{2.5}$, humidity and temperature from the Hefei city during this period, correlations among the concentrations of these pollutants were analyzed. It was found that the atmospheric concentrations of NO_3 and N_2O_5 were affected by a variety of atmospheric conditions during a rapid atmospheric cleaning event in the winter of 2017.

V. ACKNOWLEDGMENTS

Hao Wu, Jian Chen, An-wen Liu, and Shui-ming Hu acknowledge the supports from the Ministry of Science and Technology of China (No.2013BAK12B00), and the National Natural Science Foundation of China (No.21427804).

DOI:10.1063/1674-0068/cjcp1910173

[1] B. J. Allan, N. Carslaw, H. Coe, R. A. Burgess, and J. M. C. Plane, J. Atmos. Chem. **33**, 129 (1999).
[2] S. S. Brown and J. Stutz, Chem. Soc. Rev. **41**, 6405 (2012).
[3] J. L. Fry, D. C. Draper, K. C. Barsanti, J. N. Smith, J. Ortega, P. M. Winkler, M. J. Lawler, S. S. Brown, P. M. Edwards, R. C. Cohen, and L. Lee, Environ. Sci. Technol. **48**, 11944 (2014).
[4] R. Atkinson, D. L. Baulch, R. A. Cox, J. N. Crowley, R. F. Hampson, R. G. Hynes, M. E. Jenkin, M. J. Rossi, J. Troe, and T. J. Wallington, Atmos. Chem. Phys. **8**, 4141 (2008).
[5] W. L. Chang, P. V. Bhave, S. S. Brown, N. Riemer, J. Stutz, and D. Dabdub, Aerosol Sci. Technol. **45**, 655 (2011).
[6] F. J. Dentener and P. J. Crutzen, J. Geophys. Res. **98**, 7149 (1993).
[7] D. Hanway and F. M. Tao, Chem. Phys. Lett. **285**, 459 (1998).
[8] S. S. Brown, J. A. Neuman, T. B. Ryerson, M. Trainer, W. P. Dubé, J. S. Holloway, C. Warneke, J. A. de Gouw, S. G. Donnelly, E. Atlas, B. Matthew, A. M. Middlebrook, R. Peltier, R. J. Weber, A. Stohl, J. F. Meagher, F. C. Fehsenfeld, and A. R. Ravishankara, Geophys. Res. Lett. **33**, L08801 (2006).
[9] N. Riemer, H. Vogel, B. Vogel, B. Schell, I. Ackermann, C. Kessler, and H. Hass, J. Geophys. Res. D Atmos. **108**, 5 (2003).
[10] A. Geyer, B. Alicke, R. Ackermann, M. Martinez, H. Harder, W. Brune, P. Di Carlo, E. Williams, T. Jobson, S. Hall, R. Shetter, and J. Stutz, J. Geophys. Res. Atmos. **108**, 4368 (2003).
[11] J. F. Noxon, R. B. Norton, and W. R. Henderson, Geophys. Res. Lett. **91**, 5323 (1978).
[12] J. P. Kercher, T. P. Riedel, and J. A. Thornton, Atmos. Meas. Tech. **2**, 193 (2009).
[13] D. Mihelcic, D. Klemp, P. Müsgen, H. W. Pätz, and A. Volz-Thomas, J. Atmos. Chem. **16**, 313 (1993).
[14] A. Geyer, B. Alicke, D. Mihelcic, J. Stutz, and U. Platt, J. Geophys. Res. Atmos. **104**, 26097 (1999).
[15] J. Matsumoto, H. Imai, N. Kosugi, and Y. Kajii, Atmos. Environ. **39**, 6802 (2005).
[16] T. Wagner, C. Otten, K. Pfeilsticker, I. Pundt, and U. Platt, Geophys. Res. Lett. **27**, 3441 (2000).
[17] R. B. Norton and J. F. Noxon, J. Geophys. Res. **91**, 5323 (1986).
[18] U. Platt, J. Meinen, D. Pöhler, and T. Leisner, Atmos. Meas. Tech. **3**, 127 (2010).
[19] R. M. Varma, D. S. Venables, A. A. Ruth, U. Heitmann, E. Schlosser, and S. Dixneuf, Appl. Opt. **18**, B159-71 (2009).
[20] M. Baasandorj, S. W. Hoch, R. Bares, J. C. Lin, S. S. Brown, D. B. Millet, R. Martin, K. Kelly, K. J. Zarzana, C. D. Whiteman, W. P. Dube, G. Tonnesen, I. C. Jaramillo, and J. Sohl, Environ. Sci. Technol. **51**, 5941 (2017).
[21] Z. Li, R. Hu, P. Xie, H. Wang, K. Lu, and D. Wang, Sci. Total Environ. **613-614**, 131 (2018).
[22] S. Wang, C. Shi, B. Zhou, H. Zhao, Z. Wang, S. Yang, and L. Chen, Atmos. Environ. **70**, 401 (2013).
[23] Z. Li, R. Hu, P. Xie, H. Chen, S. Wu, F. Wang, Y. Wang, L. Ling, J. Liu and W. Liu, Opt. Express. **26**, A433 (2018).
[24] X. Wang, T. Wang, C. Yan, Y. J. Tham, L. Xue, Z. Xu, and Q. Zha, Atmos. Meas. Tech. **7**, 1 (2014).
[25] J. Chen, H. Wu, A. W. Liu, S. M. Hu, and J. Zhang, Chin. J. Chem. Phys. **30**, 493 (2017).
[26] W. P. Dubá, S. S. Brown, H. D. Osthoff, M. R. Nunley, S. J. Ciciora, M. W. Paris, R. J. McLaughlin, and A. R. Ravishankara, Rev. Sci. Instrum. **77**, 034101 (2006).
[27] H. Fuchs, W. P. Dubé, S. J. Ciciora, and S. S. Brown, Anal. Chem. **80**, 6010 (2008).
[28] H. D. Osthoff, M. J. Pilling, A. R. Ravishankara, and S. S. Brown, Phys. Chem. Chem. Phys. **9**, 5785 (2007).
[29] I. E. Gordon, L. S. Rothman, C. Hill, R. V. Kochanov, Y. Tan, P. F. Bernath, M. Birk, V. Boudon, A. Campargue, K. V. Chance, B. J. Drouin, J. M. Flaud, R. R. Gamache, J. T. Hodges, D. Jacquemart, V. I. Perevalov, A. Perrin, K. P. Shine, M. A. H. Smith, J. Tennyson, G. C. Toon, H. Tran, V. G. Tyuterev, A. Barbe, A. G. Császár, V. M. Devi, T. Furtenbacher, J. J. Harrison, J. M. Hartmann, A. Jolly, T. J. Johnson, T. Karman, I. Kleiner, A. A. Kyuberis, J. Loos, O. M. Lyulin, S. T. Massie, S. N. Mikhailenko, N. Moazzen-Ahmadi, H. S. P. Mller, O. V. Naumenko, A. V. Nikitin, O. L. Polyansky, M. Rey, M. Rotger, S. W. Sharpe, K. Sung, E. Starikova, S. A. Tashkun, J. Vander Auwera, G. Wagner, J. Wilzewski, P. Wcisło, S. Yu, and E. J. Zak, J. Quant. Spectrosc. Radiat. Transf. **203**, 3 (2017).
[30] V. Gorshelev, A. Serdyuchenko, M. Weber, W. Chehade, and J. P. Burrows, Atmos. Meas. Tech. **7**, 609 (2014).
[31] S. P. Sander, R. R. Friedl, D. M. Golden, M. J. Kurylo, G. K. Moortgat, P. H. Wine, A. R. Ravishankara, C. E. Kolb, M. J. Molina, S. Diego, L. Jolla, R. E. Huie, and V. L. Orkin, *Chemical Kinetics and Photochemical Data for Use in Atmospheric Studies: Evaluation Number 17*, JPL Publication, 10-06 (2006).
[32] W. B. Demore, J. J. Margitan, M. J. Molina, R. T. Watson, D. M. Golden, R. F. Hampson, M. J. Kurylo, C. J. Howard, and A. R. Ravishankara, Int. J. Chem. Kinet. **17**, 1135 (1985).

DOI:10.1063/1674-0068/cjcp1910173